Molecular Microbiology (2014) 92(2), 302–315 ■
doi:10.1111/mmi.12557
First published online 14 March 2014

Identification of *in vivo* regulators of the *Vibrio cholerae xds* gene using a high-throughput genetic selection

EmilyKate McDonough, David W. Lazinski and Andrew Camilli*
Howard Hughes Medical Institute and Department of Molecular Biology and Microbiology, Tufts University School of Medicine, Boston, MA 02111, USA.

Summary

***Vibrio cholerae*, the causative agent of cholera, remains a threat to public health in areas with inadequate sanitation. As a waterborne pathogen, *V. cholerae* moves between two dissimilar environments, aquatic reservoirs and the intestinal tract of humans. Accordingly, this pathogen undergoes adaptive shifts in gene expression throughout the different stages of its lifecycle. One particular gene, *xds*, encodes a secreted exonuclease that was previously identified as being induced during infection. Here we sought to identify regulators responsible for the *in vivo*-specific induction of *xds*. A transcriptional fusion of *xds* to two consecutive antibiotic resistance genes was used to select transposon mutants that had inserted within or adjacent to regulatory genes and thereby caused increased expression of the *xds* fusion under non-inducing conditions. Large pools of selected insertion sites were sequenced in a high throughput manner using Tn-seq to identify potential mechanisms of *xds* regulation. Our selection identified the two-component system PhoB/R as the dominant activator of *xds* expression. *In vitro* validation confirmed that PhoB, a protein which is only active during phosphate limitation, was responsible for *xds* activation. Using *xds* expression as a biosensor of the extracellular phosphate level, we observed that the mouse small intestine is a phosphate-limited environment.**

Introduction

Vibrio cholerae, the causative agent of the severe diarrhoeal disease cholera, is a model organism for the study of waterborne facultative pathogens. *V. cholerae* is a natural member of temperate aquatic environments around the world and is often found in biofilms associated with phyto- and zooplankton (Lipp *et al.*, 2002). The bacteria enter the human host via ingestion of contaminated water and colonize the small intestine. The process of colonization leads to the induction of the ToxR virulence gene regulon and consequently the production of cholera toxin (CT) and CT induced secretory diarrhoea (Peterson, 2002). The bacteria are shed from the human host via diarrhoea back into the environment where they can persist until once again ingested by a host.

Because *V. cholerae* inhabits two dissimilar niches, aquatic environments and the human intestinal tract, it must undergo adaptive shifts in gene expression throughout the various stages of its lifecycle (e.g. DiRita, 1992; Merrell *et al.*, 2002; Nielsen *et al.*, 2006; Childers and Klose, 2007; Schild *et al.*, 2007; Nielsen *et al.*, 2010). These dramatic shifts in gene expression are essential for survival of the organism when exposed to extreme environments such as the acidic human stomach and the nutrient poor aquatic environment. The *V. cholerae* virulence gene regulatory cascade, which is induced within the first few hours of infection in the infant mouse model host (Lee *et al.*, 1999), has been well characterized (Kovacikova and Skorupski, 2002; Miller *et al.*, 2002; Zhu *et al.*, 2002; Zhu and Mekalanos, 2003; Nielsen *et al.*, 2006; Childers and Klose, 2007). However, we are only beginning to understand changes in this pathogen at later stages of infection.

Following colonization and multiplication of *V. cholerae* in the rabbit ileal loop model of infection, the bacteria undergo the 'mucosal escape response' during which the bacteria detach from the mucus-lined intestinal epithelia and move into the lumen, preparing for exit from the host. A major characteristic of the mucosal escape response is large shifts in gene expression, which are co-ordinated by the major quorum sensing regulator, HapR, and the stress response alternative sigma factor, RpoS (Nielsen *et al.*, 2006; 2010). Using the infant mouse model, our laboratory identified 57 *V. cholerae* 'late' genes whose expression is induced after virulence gene induction, but not during growth *in vitro* in a rich medium. Specifically, late genes were described as genes whose expression

Accepted 17 February, 2014. *For correspondence. E-mail Andrew.camilli@tufts.edu; Tel. (+1) 617 636 2144; Fax (+1) 617 636 2175.

increases ≥ 2-fold between either the 5-hour or 7-hour and 21-hour time point of infection of an infant mouse (Schild *et al*., 2007). Several of these late genes were implicated in preparing the bacteria for transition to the aquatic environment, rather than contributing to colonization or virulence of the pathogen. Ten of the late genes are under control of RpoS, although six are known to be repressed by this alternative sigma factor (Nielsen *et al*., 2006). Thus, the transcriptional induction of late genes is likely to be complex. It is possible that RpoS, in combination or competition with other transcription factors, plays an important role in regulating some of the late genes. However, not all of the late genes are under the control of RpoS, and therefore we hypothesize that there exist different subgroups of late genes that are under the control of different global regulatory networks.

We were interested in learning more about how *V. cholerae* regulates the transcription throughout infection. One gene of interest, which was originally identified as a late gene, is *xds* (VC2621). *xds* encodes one of two secreted DNases produced by *V. cholerae*, the other being Dns (Newland *et al*., 1985; Focareta and Manning, 1987; 1991a,b). Xds has exonuclease activity, while Dns exhibits endonuclease activity (Seper *et al*., 2011). Despite the fact that *xds* was independently shown to be induced during both infant mouse and human infection (Lombardo *et al*., 2007; Schild *et al*., 2007), deletion of *xds* does not result in attenuation of virulence (Focareta and Manning, 1991a). Therefore, the role of Xds during infection, if any, is unclear. It is conceivable that Xds plays a role in degrading the DNA component of mucus in the small intestine in order to promote mucosal escape. Interestingly, both secreted nucleases have been shown to degrade DNA found in neutrophil extracellular traps (NETS), suggesting they may contribute to evasion of the innate immune system, although the contribution of Xds to this phenotype is minimal (Seper *et al*., 2013). On the other hand, recent work has demonstrated a role for Xds outside the host, where it modulates biofilm development and dissolution on abiotic surfaces (Seper *et al*., 2011).

In hopes of gaining more insight into a possible role for Xds during infection, as well as the *in vivo* inducing signal for *xds* transcription, we set out to identify the transcriptional regulator(s) of *xds*. To this end, we designed a genetic selection that couples a traditional antibiotic selection with high-throughput transposon sequencing (Tn-seq). Using this genetic selection, we identified the phosphate starvation, two-component regulatory system PhoB/R as the dominant activator of *xds*. We validated this regulatory connection both *in vitro* and *in vivo* (during infection). Furthermore, we have provided evidence that the mouse small intestine is a low phosphate environment capable of triggering PhoB/R activity.

Results

Design of a high-throughput genetic selection to identify regulators of xds

In designing the genetic selection outlined in Fig. 1, we took advantage of the fact that *xds* is induced during infection, but not during growth in Luria–Bertani (LB) broth (Schild *et al*., 2007). To this end, we made a transcriptional fusion of the normally monocistronic *xds* to two antibiotic resistance markers: *bla*, encoding carbenicillin (Cb) resistance, and *neo*, encoding kanamycin (Kn) resistance in the *V. cholerae* O1 El Tor strain E7946. The resulting strain containing the *xds–bla–neo* fusion was subjected to mTn*10* transposon mutagenesis. For this we designed a new, highly efficient mTn*10* delivery plasmid (pDL1098) for performing mutagenesis, which is described in Experimental Procedures and Fig. S1. The mTn*10* carries *lacI* together with an isopropyl β-D-1-thiogalactopyranocide (IPTG) inducible outward-reading P_{tac} promoter. The transposon mutant library was plated on LB agar supplemented with Cb + Kn (± IPTG) to select for transposon insertions that caused enhanced expression of *xds–bla–neo*. Three independent selections were performed using slightly different antibiotic concentrations, however the results were highly similar for each selection. We therefore considered each of the three antibiotic conditions to be essentially equivalent biological replicates.

The presence and absence of IPTG during selection allowed for the identification of both activators and repressors. Transposon insertions that disrupted an *xds* repressor would enhance expression of *xds–bla–neo*. These transposon insertion mutants would be enriched in either the presence or absence of IPTG. Alternatively, elevated expression of *xds–bla–neo* could occur in the presence of IPTG when the outward reading promoter of the transposon drove expression of an activator.

We used Tn-seq to identify transposon insertions enriched in our selection (van Opijnen *et al*., 2009). Since Tn-seq identifies all transposon insertions present in the selection pool, and the frequency at which they are present, we hypothesized that Tn-seq would allow us to identify both strong and weak transcriptional regulators. Tn-seq also allowed for accurate determination of the complexity of our input transposon library, which was 169198 unique insertions representing insertions in 3526 of 3885 annotated open reading frames (ORFs) in the *V. cholerae* genome. The remaining 359 ORFs (9%) that were not disrupted correlated well with the essential gene lists previously described (Cameron *et al*., 2008; Chao *et al*., 2013; Kamp *et al*., 2013), indicating that our library was at or very near saturation.

We developed methods of data analysis specific to this technique, in order to determine transposon insertions that were significantly enriched. We analysed the + IPTG

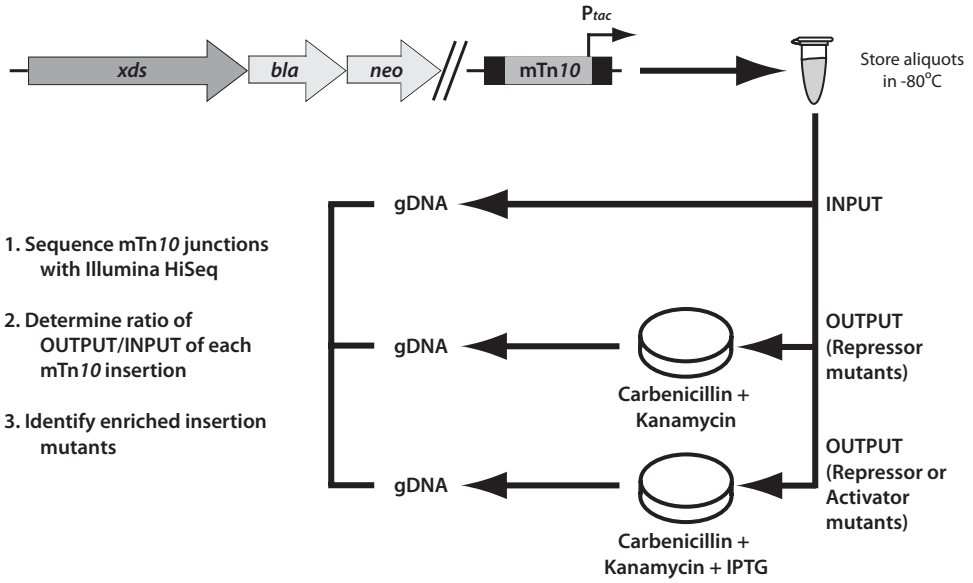

Fig. 1. Outline of genetic selection for regulators of *xds*. *xds* was transcriptionally fused to the beta-lactamase (*bla*) and neomycin phosphotransferase (*neo*) genes, which encode resistance to carbenicillin and kanamycin respectively. As an *in vivo* induced gene, *xds* is expressed at low levels during growth on LB agar, therefore, the fusion strain (*xds–bla–neo*) is carbenicillin/kanamycin sensitive on plates. *xds–bla–neo* was mutagenized with a mini-Tn*10* transposon, which carries an outward reading, IPTG-inducible promoter, P_{tac}. Mutants with increased expression of *xds–bla–neo* were selected on either carbenicillin + kanamcyin or carbenicillin + kanamycin + 1 mM IPTG. Transposon insertions enriched on the plates without IPTG were those disrupting a repressor of *xds*. Conversely, transposon insertions enriched under IPTG positive conditions included both repressor knock-outs and insertions upstream of *xds* activators. After selection, genomic DNA (gDNA) was isolated from pooled colonies and the samples were prepared for transposon junctional sequencing using the Illumina HiSeq. Input gDNA was prepped directly from the frozen transposon libraries.

and -IPTG selection data separately and differently because the type of transposon insertion mutation we were interested in was different for each condition (insertions upstream of activators versus insertions within repressors). A detailed description of the data analysis is provided in the Experimental Procedures.

In order to identify repressors of *xds*, we utilized the -IPTG selection data. From this data, we calculated a fold enrichment score for each gene (FE_{gene}) in all three antibiotic selection outputs. An average FE_{gene} of the three independent selections was calculated. The resulting FE_{gene} averages indicated a high degree of separation between enriched and non-enriched genes (Table S1). Using this method we identified five repressors of *xds*: *pstS-1*, *pstC-1*, *pstA-1* and *phoU* (Table 1). Additionally, we performed statistical analysis using the Wilcoxon signed-rank test with a Bonferroni correction for multiple comparisons on the -IPTG data. The test compared read counts in the output to those, paired by insertion site, in the input, for each gene separately. For both fold enrichment scores and Wilcoxon signed-rank test results, the results unambiguously distinguished regulator genes from background genes (Table S1). The five putative repressor genes identified via FE_{gene} scores (Table 1) were the only

Table 1. Putative repressors identified in the absence of IPTG.

Locus[a]	Gene annotation/symbol[a]	Fold enrichment[b]	Wilcoxon signed-rank test *P*-value
VC0721	Phosphate ABC transporter, periplasmic phosphate-binding protein (*pstS-1*)	1710	5×10^{-19}
VC0724	Phosphate ABC transporter, permease protein (*pstC-1*)	3559	1×10^{-32}
VC0725	Phosphate ABC transporter, permease protein (*pstA-1)*	2679	4×10^{-27}
VC0726	Phosphate ABC transporter, ATP-binding protein (*pstB-1*)	2648	2×10^{-14}
VC0727	Phosphate transport system regulatory protein PhoU (*phoU*)	2738	3×10^{-7}

a. Gene locus and gene annotation/symbol are listed according to the JCVI Comprehensive Microbioal Resource database (http://cmr.jcvi.org/cgi-bin/CMR/CmrHomePage.cgi).
b. FE_{gene}.

Table 2. Putative activators identified in the presence of IPTG.

Insertion position	Locus affected by insertion	Gene annotation/symbol[a]	Fold enrichment[b]
Chr I 773094	VC0720	Histidine protein kinase PhoR (*phoR*)	174
Chr I 773222	VC0720	Histidine protein kinase PhoR (*phoR*)	1722

a. Gene locus and gene annotation/symbol are listed according to the JCVI Comprehensive Microbioal Resource database (http://cmr.jcvi.org/cgi-bin/CMR/CmrHomePage.cgi).
b. $FE_{insertion}$.

genes exhibiting statistical significance using the Wilcoxon signed-rank test.

The proteins encoded by *pstS-1*, *pstC-1*, *pstA-1*, *pstB-1* and *phoU* are part of the Pst/PhoU system, which is an ABC transporter of inorganic phosphate. Although the mechanism is unclear, Pst/PhoU also regulates the activity of the PhoB/R two-component system in response to the extracellular phosphate level. Under high phosphate conditions, Pst/PhoU inhibits autophosphorylation of the histidine kinase PhoR and thus represses activity of PhoB and expression of the Pho regulon. Under low phosphate conditions, PhoB/R is active and induces transcription of low phosphate response genes (Lamarche *et al*., 2008). Null mutations in the Pst/PhoU system of *V. cholerae*, such as our enriched transposon insertions, mimic the low phosphate state resulting in constitutive activation of PhoB (Pratt *et al*., 2009).

To identify putative activators of *xds* we analysed the + IPTG selection data. The genes of interest in the + IPTG selection are downstream of the transposon-carried P_{tac} promoter. Instead of examining the + IPTG data on the gene level, as we had done for the -IPTG data, we analysed the data at the insertion level. This analysis allowed us to identify enriched insertions, determine their directionality, and examine which downstream genes were potentially affected. Insertions were ranked by fold enrichment ($FE_{insertion}$) as described in Experimental Procedures. Insertions of interest were those that exhibited $FE_{insertion}$ greater than five, but were not directly upstream of the *bla-neo* fusion or in the coding or promoter regions of genes identified in the -IPTG selection (Table S2). Finally, we only considered genes having two or more enriched insertions in the upstream gene and/or intergenic region that were oriented in the same direction.

We identified two insertions in the 5′ end of *phoR* that were enriched (Table 2 and Fig. 2). The first insertion was located at 117 bp downstream of the initiator AUG and was enriched 174-fold. The other insertion, located at base pair 245, was enriched 1722-fold. In both cases the transposon was oriented such that its P_{tac} promoter could drive expression of a 5′-truncated *phoR* gene in an IPTG-dependent manner. Although there were 57 insertions in both orientations throughout the *phoR* coding sequence in our input transposon library, we only identified these two insertions enriched in the output. Using the domain prediction algorithms built into BLAST (NCBI), we determined that both transposon insertions could promote expression of truncated PhoR proteins that lack their periplasmic and transmembrane domains but still contain all domains thought to be important for phosphotransfer. In the more highly enriched mutant, an in-frame initiator codon was created at the transposon-chromosome junction. We

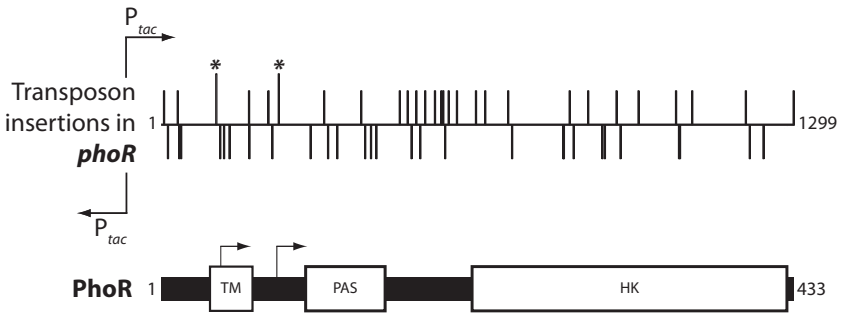

Fig. 2. Transposon insertions in *phoR*. Each vertical line indicates the position of a single transposon insertion in the coding region of *phoR*. Lines above *phoR* indicate that the orientation of the transposon carried P_{tac} promoter is the same as that of P_{phoR} and the converse is true of the lines below *phoR*. Two transposon insertions were selected specifically in the selection done in the presence of IPTG, these insertions are indicated by asterisks in the upper diagram and by the two arrows in the lower diagram. The predicted domain structure of PhoR is also provided: TM – predicted transmembrane domain (12–34 a.a.), PAS – Per/Arnt/Sim domain (99–153 a.a.), and HK – Histidine kinase domain (205–427 a.a.). Transcription from the P_{tac} promoter carried on the enriched transposons would lead to expression of truncated PhoR proteins, each lacking a functional transmembrane domain.

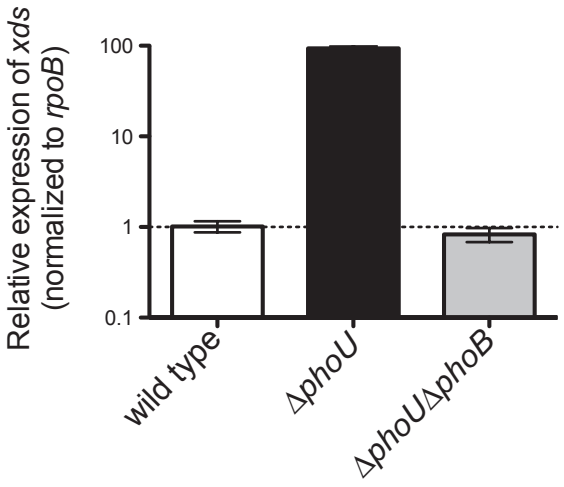

Fig. 3. Expression of *xds* was measured in wild type, Δ*phoU*, Δ*phoU*Δ*phoB* strains using qRT-PCR. Transcript levels were normalized to the housekeeping gene *rpoB*, and set relative to the wild type strain. Bacteria were grown on LB agar plates at 37°C for 2 h to mimic selection conditions. Bacteria were subsequently removed from the plates and RNA was isolated. Four biological replicates are represented for each strain. Mean and standard deviation are shown.

hypothesize that expression of PhoR without its transmembrane domain leads to constitutive activation of the sensor kinase likely by removing the protein from the membrane and therefore preventing its interaction with the membrane-bound Pst/PhoU inhibitor complex.

In vitro *validation of selection results*

To validate repressor activity of Pst/PhoU on *xds* we performed quantitative reverse transcriptase-polymerase chain reaction (qRT-PCR) on *xds* transcripts. We compared transcript level in wild type cells to that in a Δ*phoU* background (Fig. 3). We reasoned that deletion of *phoU* should have the same effect as deleting any of the other *pst* genes, resulting in constitutive activation of PhoB. In order to closely mimic the conditions of our genetic selection, we collected RNA for these experiments from LB agar plate grown bacteria. In support of our selection results, deletion of *phoU* resulted in an increase of *xds* expression (mean relative expression = 93.8-fold; SD = 7.6), when compared with wild type (mean relative expression = 1.02-fold; SD = 0.14). Furthermore, when we deleted *phoB* in the Δ*phoU* background, expression of *xds* was restored to the wild type level (mean relative expression = 0.83-fold; SD = 0.15), confirming that the *phoU* and *phoB* are epistatic. Together, these results support our selection results that PhoU is a repressor of *xds*, and that repression activity is dependent on the presence of the PhoB response regulator.

Since PhoB is active under low phosphate conditions, we hypothesized that *xds* would be induced in a phosphate-limiting environment when compared with growth in phosphate replete conditions. Recently, induction of *xds* under phosphate limiting conditions was reported in another *V. cholerae* El Tor strain, C6709 (Seper *et al.*, 2011). These authors assayed expression of *xds* under high and low phosphate conditions using an *xds–phoA* transcriptional fusion reporter strain and measured alkaline phosphatase levels as a read-out for *xds* transcription. These results are confounded by the fact that *V. cholerae* has its own functional alkaline phosphatase that is regulated by PhoB (Majumdar *et al.*, 2005; Pratt *et al.*, 2010). Therefore, under low phosphate conditions, the combined activity of the endogenous phosphatase and the reporter fusion was measured, and the relative contribution of each gene to the final readout was not assessed. Here, we used qRT-PCR to directly measure transcript levels of *xds* in high and low phosphate conditions. We grew wild type *V. cholerae* in MOPS minimal media supplemented with 10 mM (high) or 0.1 mM (low) KH_2PO_4 as a phosphate source. As expected, we found that *xds* was induced under low phosphate conditions in the wild type background (mean relative expression = 61.1-fold; SD = 2.4), when compared with growth in replete phosphate (mean relative expression = 1.01-fold; SD = 0.42) (Fig. 4). When we deleted *phoB*, expression of *xds* in low phosphate conditions dropped back to the level of *xds* expression seen in the wild type when it was grown in high phosphate (mean

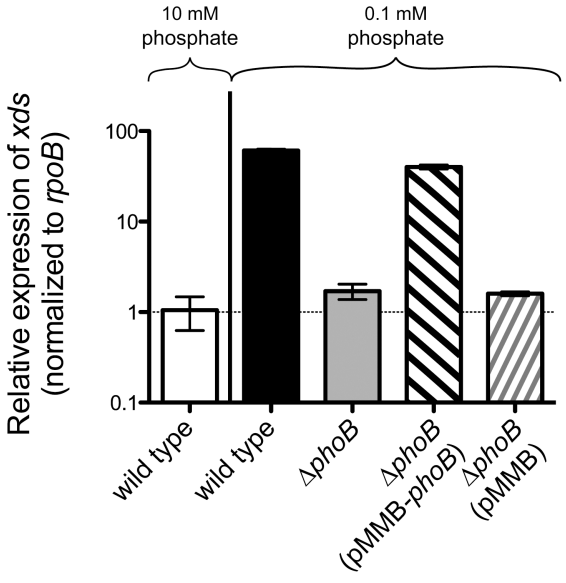

Fig. 4. The level of *xds* transcript was measured in various *V. cholerae* strains. Three biological replicates of each strain were grown overnight in MOPS media supplemented with either 10 mM or 0.1 mM KH_2PO_4 (phosphate). For plasmid containing strains, 1 mM IPTG was used to induce expression from the P_{tac} promoter. The mean and standard deviation are shown.

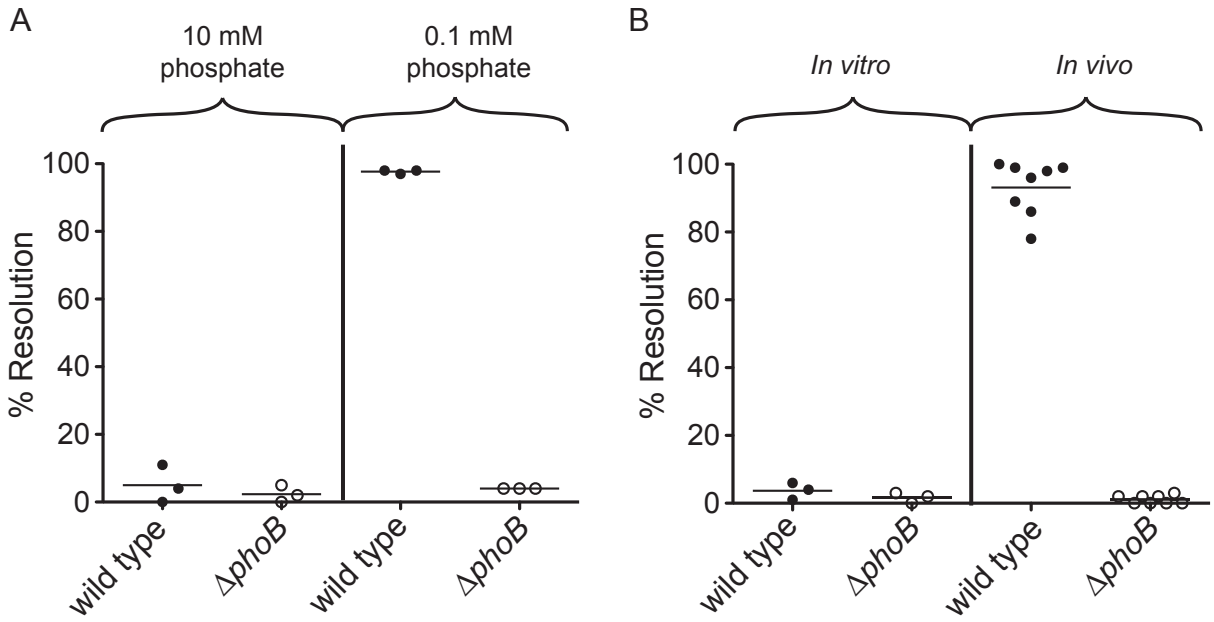

Fig. 5. Expression of *xds* was measured in the wild type (filled in circles) and Δ*phoB* (open circles) strains using RIVET.
A. Resolution of the *res* cassette was determined after 4 h of growth in MOPS media supplemented with 10 mM or 0.1 mM KH_2PO_4 (phosphate).
B. Resolution of the *res* cassette was measured after 4 h of growth in LB (*in vitro*) or 24 h post infection of an infant mouse (*in vivo*). Each data point represents the resolution frequency from either an individual culture tube or mouse. The black bars indicate the mean resolution.

relative expression = 1.70-fold; SD = 0.33). Expression of *xds* under 0.1 mM phosphate in the absence of *phoB* was complemented using expression of *phoB* from the P_{tac} promoter on the pMMB67EH vector (mean relative expression = 40.2-fold; SD = 2.1), but not using the vector alone (mean relative expression = 1.60-fold; SD = 0.07). These results further support our hypothesis that expression of *xds* is induced in phosphate limiting conditions, and transcription of *xds* depends on the presence of activated PhoB.

In vivo *validation of selection results*

We used an *in vitro* selection to identify regulators of *xds*, a gene that is only induced *in vivo*. Thus, an essential aspect of our study was to validate that any regulator identified *in vitro* was indeed important during infection. Theoretically, a repressor (e.g. *phoU*) could be overexpressed to block late gene expression, whereas an activator (e.g. *phoB*) could be deleted to prevent late induction. However, because overexpression of a *V. cholerae* gene during infection is not trivial, we chose to delete the *xds* activator implicated by our results, *phoB*, and observe the effect on *xds* transcription during infection. We used recombination-based *in vivo* expression technology (RIVET) to semi-quantitatively measure transcription of *xds* during infection of an infant mouse (Camilli and Mekalanos, 1995). The gene *tnpR*, which encodes a *res*-site specific recombinase, was transcriptionally fused to *xds*, in a strain also harbouring a TnpR substrate, the resolvable kanamycin-resistance marked cassette (*res–neo–sacB–res*) (Osorio *et al.*, 2005). When *xds* is induced in the fusion strain, TnpR is coexpressed and mediates resolution of the cassette, resulting in the loss of Kn resistance. Therefore, the strain remains resistant to Kn so long as *xds* is not induced, but becomes sensitive to Kn upon induction of *xds* and resolution of the *res* cassette.

As a test of our RIVET strains, and as further confirmation of our qRT-PCR results, we first measured resolution mediated by the *xds–tnpR* fusion in MOPS media supplemented with high or low phosphate (Fig. 5A). Resolution of the *res* cassette in the wild type strain was low in high phosphate (mean = 5.0%; SD = 5.6) and high in low phosphate (mean = 97.67%; SD = 0.58). Conversely, when we deleted *phoB*, the *res* cassette was no longer induced in low phosphate (mean = 4.0%; SD = 0), when compared with high phosphate (mean = 2.3%; SD = 2.5). These results confirmed our qRT-PCR results and demonstrated that regulation of *xds* by PhoB can be measured using RIVET.

Next, we tested resolution of the *res* cassette in the wild type and Δ*phoB* RIVET strains during infection of infant mice (Fig. 5B). To ensure that resolution was not occurring during preparation of the inocula, we first measured resolution in both of these strains grown in LB broth (the media used to grow the inocula). Neither the wild type

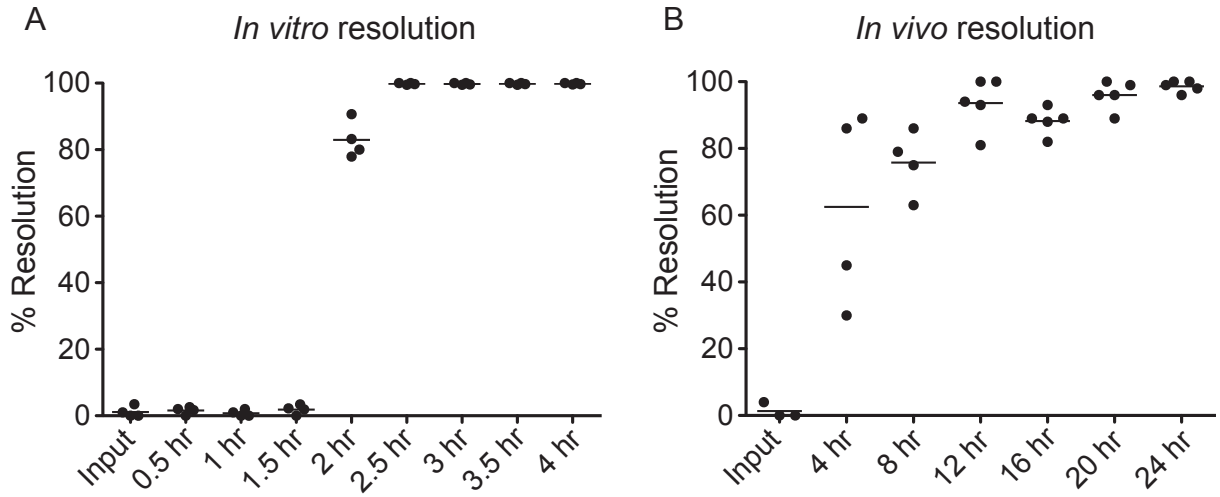

Fig. 6. Expression of *xds* was measured using RIVET after transfer of bacteria from a high phosphate medium (LB) to either (A) MOPS minimal medium lacking phosphate or (B) an infant mouse gastrointestinal tract. Each dot represents a single mouse or culture. Black bars represent the mean resolution for each time point.

RIVET (mean = 3.7%; SD = 2.5) nor the Δ*phoB* RIVET (mean = 1.7%; SD = 1.5) strains exhibited appreciable resolution in LB. When the wild type RIVET strain was passaged through an infant mouse, nearly all colony-forming units (CFU) recovered from the small intestine at 24 h had resolved the cassette (mean = 93%; SD = 8.0), consistent with *xds* being induced *in vivo*. Resolution did not occur in the Δ*phoB* RIVET strain after passage *in vivo* (mean = 1.1%; SD = 1.2). Therefore, PhoB appears to be an essential regulator of *xds* during infection.

Activation of PhoB during infection

Since *xds* is both a PhoB regulated gene and *in vivo*-induced, we hypothesized that *V. cholerae* encounters low phosphate conditions in the infant mouse small intestine. Although others have provided some evidence that PhoB and the phosphate starvation response are important during infection (von Kruger *et al*., 1999) we were interested in specifying at what time during infection phosphate becomes limiting. Our RIVET data suggested that PhoB is the dominant regulator of *xds* during infection of an infant mouse (Fig. 5B), as demonstrated by the evidence that deletion of *phoB* nearly completely prevented resolution of the *res* cassette. This conclusion was also supported by the results obtained from our Tn-seq selection where only insertions that resulted in PhoB activation were found to significantly enhance expression from the *xds* promoter. Therefore, we reasoned that PhoB activation, and thus low phosphate levels, could be measured during infection of an infant mouse by using the *xds* RIVET strain as a biosensor for phosphate.

The RIVET expression profile of *xds* described by Schild *et al*. (2007) suggested that *xds* is induced late, implying, based on our work presented here, that phosphate becomes limiting late in infection. However, we had observed, *in vitro*, that *xds* expression in a phosphate depleted medium, as measured by RIVET, is delayed when using plate grown bacteria, rather than mid-exponential phase broth grown bacteria, as the inoculum (data not shown). Since Schild *et al*. (2007) did not use mid-exponential phase bacteria, nor was care taken to exclude exogenous phosphate from the inoculum, it remains a possibility that *xds* is induced earlier during infection in response to phosphate limitation in the small intestine.

We designed an *in vivo* RIVET experiment tailored to specifically identify when phosphate becomes limiting in the infant mouse during infection. We used mid-exponential phase bacteria, washed twice, and resuspended in MOPS medium (no phosphate) as the inoculum. Prior to performing the *in vivo* experiment, we first measured expression of the RIVET inoculum over time, after transfer to MOPS medium lacking phosphate (Fig. 6A). We observed a lag of resolution of the *res* cassette of 2–2.5 h after transfer to the phosphate-depleted condition. These results suggested that the soonest we would be able to detect resolution of the cassette *in vivo* would be 2 h post inoculation. We measured resolution of the *res* cassette at 4, 8, 12, 16, 20 and 24 h post inoculation of infant mice with the RIVET strain (*xds–tnpR lacZ*::*res–sacB–neo–res*) (Fig. 6B). We found that expression the gene within the population began by 4 h, and by 12 h nearly the entire population had resolved. Interestingly, the 4 h time-point exhibited a bifurcation in the population in terms of *xds*

expression; two of the mice exhibited ~ 38% resolution at 4 h post inoculation, whereas the other two mice exhibited ~ 88% resolution. The reasons for this bifurcation phenotype are unknown. From this experiment, we conclude that the mouse small intestine is a low phosphate environment, at least 4 h post inoculation. This low phosphate environment triggers PhoR/B activation resulting in induction of *xds* and likely other genes in the Pho regulon.

Re-evaluation of the xds in vivo *phenotype*

Previous studies with *V. cholerae* strains harbouring deletions in either *xds* alone or double deletions of *xds* and *dns* have concluded that *xds* is not important for colonization or virulence (Focareta and Manning, 1991a; Seper *et al*., 2011; 2013). Although each study was performed using a slightly different model of infection, in each case the fitness of the mutant strains was determined at the late stage of infection. According to our results *xds* is an early induced gene and, therefore, we reasoned that Xds may play a role in survival or growth (e.g. nutrient acquisition) during the early stage of colonization. If the role of *xds* at an early time point is modest, the fitness disadvantage may be recovered at later stages of infection, thus providing a possible explanation for why the published studies were unable to find a fitness defect for an *xds* deletion mutant. Furthermore, in our *in vivo* RIVET experiments we found that the manner in which the inoculum is prepared, specifically with regard to phosphate content, greatly impacts the timing of *xds* induction. At least two of the previous studies (Seper *et al*., 2011; 2013) used a high phosphate containing inoculum, which we found delays the induction of *xds*. Details of the inoculum used by the third study were not provided (Focareta and Manning, 1991a). Therefore, we hypothesized that an *xds* deletion may elicit a fitness disadvantage during an early stage of infection when the inoculum is prepared under low phosphate conditions.

To test this possibility, we compared wild type and Δ*xds* small intestinal colonization after 8 h of infection, which represents the time when most of the population has induced *xds* in our time-course experiment. The bacteria were prepared for infection as was described for the RIVET time-course experiment, except that in addition to a MOPS inoculum lacking phosphate we also included a control infection using bacteria resuspended in MOPS with 10 mM KH_2PO_4 (high phosphate). We performed single strain mouse infections in order to control for complementation *in trans* of Xds, which is a secreted factor. We did not observe a statistically significant difference in the number of recoverable colony-forming units in the mouse small intestine at 8 h post infection when comparing wild type and Δ*xds* strains, regardless of the phosphate concentration in the inoculum (Fig. 7). Therefore, we conclude that although *xds* is induced during infection, the role that the gene plays is either dispensable or redundant in our infection model.

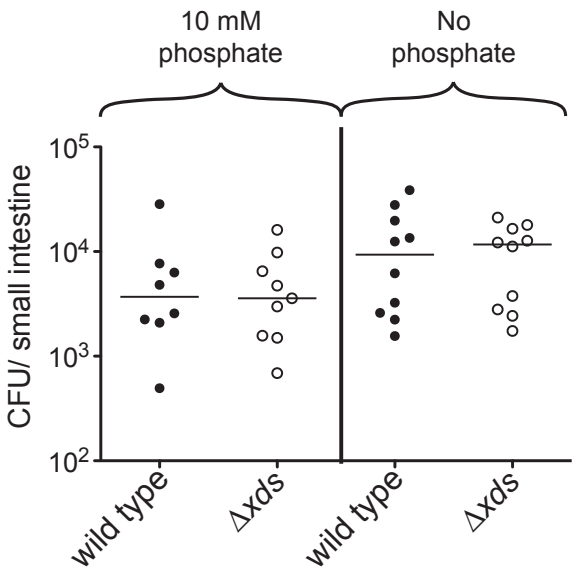

Fig. 7. The *xds* gene is not required for early colonization of the small intestine. Fitness of wild type and Δ*xds* were measured after 8 h of infection in infant mice. Each dot represents the recovered number of *V. cholerae* from a single mouse, with at least 8 mice in each group. The Mann–Whitney *U*-test was performed to compare the number of CFU per small intestine of mice colonized with either wild type or Δ*xds* strains when the inoculum was prepared in high phosphate ($P = 1.0$) or no phosphate ($P = 0.94$). The black bars represent the median values.

Discussion

As a waterborne pathogen *V. cholerae* must adapt to rapid changes in the surrounding environment. Understanding the adaptation strategies utilized by *V. cholerae* may be an important step towards controlling the pathogen. The transition of entry into the host and subsequent virulence gene expression has traditionally received more attention by researchers then have the later stages of infection or dissemination from the host. However, recently broad changes in gene expression patterns during late stages of infection and dissemination have been described using RIVET and microarray analysis (Larocque *et al*., 2005; Nielsen *et al*., 2006; 2010; Schild *et al*., 2007; Nelson *et al*., 2008). Additionally, a recent Tn-Seq study from our lab defined genes that are important for host to pond survival, using an infant rabbit model of infection (Kamp *et al*., 2013). Together, these studies have provided insight into the genetic changes of *V. cholerae* during the late stage of infection and transition to the environment.

Despite the accumulating data on the transcriptional changes that *V. cholerae* undergoes during the infection, it has been difficult to determine the precise signals that

are inducing these changes. This problem is particularly acute for signals in the host that trigger transcriptional changes in *V. cholerae* during the late stages of infection. In an attempt to determine possible inducing signals, one group used mass spectrometry to measure the levels of various metabolites present in caecal fluid collected from infected infant rabbits, as compared with metabolites present in *in vitro* culture supernatants (Mandlik *et al*., 2011). Although these metabolites do not provide a definitive list of inducing signals, they have provided information about what *V. cholerae* may be sensing (or not sensing) in the host. Phosphate levels were not reported in that study. Here, we took the alternative approach of identifying transcriptional regulators that are required for induction of a specific gene that is induced during infection. By identifying such regulators, it was our goal to uncover potential signals involved in inducing transcriptional changes within a host. We utilized a novel *in vitro* high-throughput genetic selection to identify the phosphate-responsive PhoB as the major regulator of the *V. cholerae* infection-induced gene, *xds*. Based on the timing of *xds* induction *in vivo* as described by follow-up experiments, we conclude that a low concentration of phosphate exists in the small intestine and this serves as a signal for the induction of *in vivo*-specific genes.

The qRT-PCR and RIVET experiments we performed suggest that PhoB may be the only regulator, or at least the major regulator of *xds*. It is conceivable that a weaker regulator, which does not induce expression enough to be detected by either qRT-PCR or RIVET, contributes to *xds* activation. Inconsistent with this possibility, we used high-throughput sequencing in combination with saturating transposon mutagenesis to identify all regulators of *xds*, both weak and strong, but still did not find any other regulators. If a weak regulator does exist, it is possible that we were unable to select for it because the concentration of antibiotic that we chose was too high for the low level of *xds–bla–neo* expression driven by this hypothetical weak regulator. However, this is unlikely as the concentrations of antibiotic that we used were only slightly above the level of resistance conferred by the basal level of expression of the *xds* promoter in its un-induced state.

The binding of PhoB to promoter regions has been well studied in *E. coli*, and a consensus binding site, or PhoBox, has been described (Makino *et al*., 1993; Blanco *et al*., 2011). The *xds* promoter region does not contain any sequence resembling an *E. coli* PhoBox. However, the interaction of PhoB with promoter sites in *V. cholerae* has not been well investigated. *V. cholerae* PhoB binds to three sites within the *phoBR* promoter, all of which are very similar to the *E. coli* PhoBox (Diniz *et al*., 2011). However, *V. cholerae* PhoB also interacts with a region of DNA within the *tcpPH* promoter that does not contain a putative PhoBox (Pratt *et al*., 2010). Therefore, despite the lack of an identifiable PhoBox in the *xds* promoter, PhoB may still directly bind the *xds* promoter and regulate *xds*. Since we did not identify any evidence of additional regulators of *xds* in our genetic selection, we hypothesize that PhoB is the direct regulator of *xds*. However, it is possible that the direct regulator of *xds* is essential and cannot be disrupted by transposon mutagenesis. Alternatively, there may be two or more redundantly functioning repressors of *xds*, although we surmise that such regulators would themselves be regulated by PhoB. Further studies using electro-mobility shift assays and/or promoter pull-downs could address the question of what directly regulates *xds*.

The induction of *xds* by PhoB under phosphate limiting conditions, suggests that the exonuclease, Xds, may contribute to the phosphate starvation response. Recent work has provided evidence that *V. cholerae* can utilize DNA as a phosphate source, and this ability is dependent on the presence of either *xds* or *dns* (Seper *et al*., 2011). Degradation of DNA via Xds leads to accumulation of mainly monophosphorylated nucleotides. To date, no transporter of monophosphorylated nucleotides has been identified in *V. cholerae*. Thus, it is possible that a secreted or extracellular phosphatase would work together with Xds to provide free phosphate for uptake by either Pst/PhoU or another uptake system.

Our identification of PhoB as a regulator of the infection-induced gene, *xds*, corroborates prior work that identified *pst* genes and *phoR* as transcriptionally induced during infection (Osorio *et al*., 2005; Lombardo *et al*., 2007). Additionally, dynamic activity of PhoB appears to be important during infection since deletions in *phoB* or in *pst*/*phoU*, which result in constitutively high PhoB activity, highly attenuate virulence (von Kruger *et al*., 1999; Merrell *et al*., 2002; Pratt *et al*., 2009). Here, using a RIVET-based assay, we presented evidence that PhoB is induced as soon as 4 h post infection of an infant mouse. When the same inoculum was immediately transitioned from high to no phosphate *in vitro*, there was a 2–2.5 h lag observed before this RIVET-based system could register that change. After subtracting that lag, the time post infection when a low phosphate condition was first encountered was 1.5–2 h. Given that some time is needed post infection to traverse the stomach, it is likely that as soon as bacteria reached the small intestine, they sensed a low concentration of phosphate. In other words, a low phosphate condition very likely pre-exists in the mouse small intestine prior to colonization.

Our RIVET data showing early induction of *xds* conflicts with the late induction of *xds* that was previously described (Schild *et al*., 2007). Differences between these two studies in the physiological states of the bacterial inoculum (plate grown versus mid-exponential broth grown) likely contribute to the differences in the rates of

Table 3. Strains and plasmids used in this study.

Strain or plasmid	Genotype or phenotype	Reference
Escherichia coli		
DH5α	F⁻ Δ(*lacZYA-argF*) U169 *recA1 endA1 hsdR17 supE44 thi-1 gyrA96 relA1*	Laboratory strain
DH5αλ*pir*	F⁻ Δ(*lacZYA-argF*)U169 *recA1 endA1 hsdR17 supE44 thi-1 gyrA96 relA1* λ::*pir*	Laboratory strain
SM10λ*pir*	*thi recA thr leu tonA lacY supE* RP4-2-Tc::Mu λ::*pir*, Kn^R	Laboratory strain
MFD*pir*	MG1655 RP4-2-Tc::[ΔMu1::*aac*(3)IV-Δ*aphA*-Δ*nic35*-ΔMu2::*zeo*] Δ*dapA*::(*erm*-pir) Δ*recA*	Ferrieres *et al.* (2010)
***Vibrio cholerae* strains**		
Wild type	E7946 El tor Ogawa, HapR+, Ap^R	Laboratory strain
xds–bla–neo	Transcriptional fusion of *xds* to *bla* and *neo*	This study
Δ*phoU*	In frame deletion of *phoU*	This study
Δ*phoU*Δ*phoB*	In frame deletion of *phoU* and *phoB*	This study
Δ*phoB*	In frame deletion of *phoB*	This study
Δ*phoB* (pMMB)	In frame deletion of *phoB* carrying pMMB, Ap^R	This study
Δ*phoB* (pMMB-*phoB*)	In frame deletion of phoB carrying pMMB-*phoB*, Ap^R	This study
xds RIVET	*xds–tnpR lacZ*::*res–neo–sacB–res*, Ap^R, Kn^R	This study
Δ*phoB xds* RIVET	Δ*phoB xds–tnpR lacZ*::*res–neo–sacB–res*, ApR, KnR	This study
Δ*xds*	In frame deletion of *xds*	Laboratory strain
Plasmids		
pMMB	pMMB67EH IncQ $lacI^q$ *bla* (Ap^R) P_{tac} *rrnB*	Furste *et al.* (1986)
pMMB-*phoB*	pMMB67EH with the *phoB* ORF cloned into EcoRI and BamHI restriction sites	This study
pDL1098	Temperature-sensitive mTn*10* delivery vector, Fig. S1, Cm^R, Sp^R	This study
pDL1098-flp	Temperature-sensitive Flp recombinase delivery vector, Fig. S2, Cm^R	This study
pCVD442lac	Allelic exchange vector, Fig. S3, Ap^R	Laboratory strain
pCVD442catlac	Allelic exchange vector, Fig. S4, Cm^R	Laboratory strain
pIVET-VC2621	*tnpR* delivery vector containing VC2621 (*xds*) fragment, OriR6K, Ap^R	Schild *et al.* (2007)

resolution that were observed. We hypothesize that internal phosphate stores, such as poly-phosphate, may differ between plate grown and mid-exponential phase bacteria, and that the presence of an internal phosphate store may delay activation of PhoB in a low phosphate environment. Furthermore, in contrast to this study, the inoculum used by Schild *et al*. (2007) was diluted in LB, a high phosphate-containing medium, and this likely also contributed to the delay in resolution. Finally, the ribosome binding site used by Schild *et al*. (2007) to drive TnpR translation was weaker than the one used in this study. Due to less efficient translation, more transcripts were needed to achieve the critical level of resolvase required for resolution and this undoubtedly exacerbated the observed delay. Importantly, in this study, we identified low-phosphate as the major inducer of *xds* expression and this knowledge enabled us to promote *xds* induction *in vitro*. We therefore could compare the rate of resolution of our inoculum *in vitro* with that *in vivo*, and this enabled the calibration of our RIVET-based clock. At the time of the Schild *et al*. (2007) study, there was no knowledge of *xds* regulation and *xds* induction *in vitro* could not be achieved, and therefore calibration of their RIVET-based clock was not possible.

We have described the use of a high-throughput genetic selection to identify regulators of genes that are not naturally expressed *in vitro*. Towards that end, we used Tn-seq in combination with the selection for expression of antibiotic resistance genes inserted at the non-expressed locus and, to our knowledge, this has not been done before. Although our use of this method focused on one infection-induced gene in *V. cholerae*, the method has broad application for identifying regulators of conditionally expressed genes, and could be used with any genetically tractable organism.

Experimental procedures

Media and bacterial strains

Bacterial strains were propagated in LB broth with aeration or on LB agar at 37°C, unless otherwise noted. When indicated bacteria were grown in MOPS minimal media [1× MOPS salts (40 mM MOPS pH 7.4 (3-(N-morpholino)propanesulphonic acid) (Sigma Aldrich), 4 mM tricine, 0.1 mM $FeSO_4$•$7H_2O$, 9.5 mM NH_4Cl, 0.28 mM KCl, 0.53 mM $MgCl_2$•$6H_2O$, and 50 mM NaCl); 1× NRES (25 mM of each of the amino acids N, R, E and S); 1× trace metals (0.005% $MgSO_4$, 0.0005% $MnCl_2$•$4H_2O$, 0.0005% $FeCl_3$, and 0.0004% nitrilotriacetic acid); and 0.5% glucose], supplemented with either 0.1 mM (low) or 10 mM (high) KH_2PO_4. Unless otherwise noted, antibiotics were used at the following concentrations: 100 μg ml^{-1} streptomycin (Sm), 100 μg ml^{-1} ampicillin (Ap), 2 μg ml^{-1} chloramphenicol (Cm), 50 μg ml^{-1} spectinomycin (Sp) and 50 μg ml^{-1} kanamycin (Kn). Addition of 1 mM IPTG to either plates or broth was used to induce transcription from the P_{tac} promoter.

Strains and plasmids used in this study are listed in Table 3. PCR primers used are listed in Table S3. All *V. cholerae* strains were constructed using standard molecular techniques in an Sm resistant derivative of the clinical isolate

E7946 (Mekalanos, 1983). For strain construction details, see the Supporting Information. All mutations generated in this study were confirmed by Sanger sequencing by the Tufts University Core Facility (TUCF). Plasmids were maintained in *Escherichia coli* DH5α*λpir* (*ori*R6K containing plasmids) or DH5α. Unless otherwise noted, the donor strain, *E. coli* SM10*λpir*, was used for conjugative transfer of plasmids.

Transposon mutagenesis

The mTn*10* delivery vector pDL1098 (Fig. S1) is temperature-sensitive for replication, but requires high temperature for transposition. At the permissive temperature of 30°C the plasmid replicates and the transposase is repressed. At the non-permissive temperature of 40°C the transposase is induced and replication stops, resulting in loss of the vector in the multiplying population of bacteria. For mTn*10* mutagenesis of the *V. cholerae xds–bla–neo* strain, pDL1098 was transferred into the strain via filter mating with an *E. coli* MFD*pir* mating strain (Ferrieres *et al*., 2010). Exconjugates were selected on LB agar supplemented with 2.5 μg ml^{-1} Cm and 50 μg ml^{-1} Sp and grown at 30°C. Two independent transposon libraries were made from single colonies by inoculating each into a 2 ml LB culture supplemented with 2.5 μg ml^{-1} Cm and 50 μg ml^{-1} Sp. Cultures were grown overnight at 30°C with aeration. In the morning, 0.5 ml of the turbid culture was passaged into 50 ml of LB media supplemented with 100 μg ml^{-1} Sp and pre-warmed to 40°C. After overnight, aerated growth at 40°C, 100 μl of the culture was further passaged into another 100 ml of pre-warmed LB supplemented with 100 μg ml^{-1} Sp. A second passage at 40°C in the presence of Sp was found necessary to completely eliminate bacteria harbouring the transposon delivery plasmid. The final libraries were frozen in aliquots at −80°C in 20% glycerol.

Determination of selection conditions

We performed a series of minimal inhibitory concentration (MIC) experiments to determine concentrations of Cb + Kn for our selection. In these experiments, we varied Cb and Kn concentrations, as well as the number of CFU plated. We chose antibiotic and cell density combinations as close to the MIC as possible and that fulfilled the following criteria: produced little to no background growth, allowed for development of discrete colonies, and exhibited reproducible degrees of killing. In conditions where the concentration of at least one of the antibiotics was too close to the MIC, the selection was not consistent from plate to plate in terms of both background growth and percent kill. Additionally, the freshness of the antibiotics and dryness of the selection plates contributed greatly to experiment-to-experiment variability.

A total of 6 selection conditions were chosen in order to increase the robustness of our selection for regulators of *xds*: 16 μg ml^{-1} Cb + 40 μg ml^{-1} Kn, 18 μg ml^{-1} Cb + 45 μg ml^{-1} Kn, and 20 μg ml^{-1} Cb + 50 μg ml^{-1} Kn, all ± 1 mM IPTG. When 10^6 of the un-transposed *xds–bla–neo* strain were plated on these antibiotic conditions, no colonies grew. However, when 10^6 transposon mutagenized *xds–bla–neo* were plated on these plates, an average of 700 colonies grew. The inability of the un-transposed *xds–bla–neo* strain to grow on our selection plates suggested that spontaneous mutations, which could contribute to background noise in our selection, would not be a significant problem. The fold-killing was approximately the same for each antibiotic concentration. Selection plates without IPTG exhibited an average of 4000-fold killing, whereas plates containing IPTG exhibited an average of 1552-fold killing. We found all three conditions selected for the same transposon insertions, and have thus treated the conditions as biological replicates in our analysis.

High-throughput sequencing and genetic selection

The complexity of each transposon library was determined by Tn-seq using the HTM-PCR method of preparing the samples for sequencing as described (Klein *et al*., 2012; Lazinski and Camilli, 2013), except that nested mTn*10*-specific primers, OLJ363 and OLJ385, were used. Final PCR products were cleaned using QIAquick PCR purification kit (Qiagen). The sample was sequenced on the Illumina HiSeq 2500 using the mTn*10*-specific sequencing primer OLJ386 and read from a single-end for 50 nucleotides. Primers used for barcoding samples are listed in Table S3.

For the genetic selection, one aliquot of each transposon library was thawed and mixed in order to increase the overall complexity of the final library. The pooled library was then plated on LB agar plates supplemented with Cb and Kn at predetermined concentrations. All plates used in the genetic selection were made two days prior to usage with freshly made aliquots of antibiotics and IPTG, when added. The plates were dried in a hood for 20 min and left until usage at room temperature. Approximately 1.5×10^6 CFU were plated on an average of 10 plates for each selection condition. After overnight growth at 37°C, the colonies from each selection condition were pooled and genomic DNA was isolated from approximately 5×10^9 CFU using a DNeasy Blood and Tissue Kit (Qiagen). Genomic DNA for the input sample was isolated directly from freezer stocks of the transposon libraries. Genomic DNA samples were subject to Tn-seq as above, to determine the relative frequencies of each transposon insertion in the input and post-selection (output) populations.

Illumina HiSeq data analysis

Sequence reads of transposon junctions were analysed using the TUCF Galaxy Server (Giardine *et al*., 2005; Blankenberg *et al*., 2010; Goecks *et al*., 2010). Sequence reads were trimmed of 3′ poly-C-tails as described (Klein *et al*., 2012). Low quality reads were discarded using the 'Filter by quality' script, which assigns a FASTQ quality score to each base in a single read. We retained any reads in which ≥ 95% of the bases had a quality score of > 7. Reads were mapped to the *V. cholerae* N16961 genome (GenBank Accession No. NC_002505 and NC_002506) using Bowtie. The default Bowtie parameters were used with two modifications: we required Bowtie to guarantee that each read was the best in terms of quality and stratum and we allowed Bowtie to backtrack 800 times when attempting to align a read. The TUCF custom scripts, 'hopcount' and 'aggregate hop table', were run on the mapped reads. Hopcount tallies the number of sequencing reads at every insertion site, which was used to determine the

complexity of the input library, as well as the severity of the genetic selection (i.e. we learned how many transposon insertions are represented in the output as compared with the input). Hopcount also provides directionality of the transposon and its outward reading IPTG-inducible P_{tac} promoter. Aggregate hop table totals the number of sequencing reads in each gene. Included in the aggregate hop table output is a standardized frequency of transposon insertions for every gene (standardized read frequency), corrected for the gene size and calculated by the equation: standardized read frequency = [(number of reads in gene X/total number of reads in Illumina library)/(size of gene X/total genome size)].

Enriched genes in the IPTG negative selections, which represent putative repressors of *xds*, were identified by two methods. We calculated fold enrichment for every gene (FE_{gene}), where FE_{gene} = standardized read frequency in output/standardized read frequency in input. Genes were ordered genes by their FE_{gene} score and the average FE_{gene} of the three antibiotic conditions was used to calculate the reported FE_{gene} scores. We also used the Wilcoxon signed-rank test as calculated by the JMP statistics software package (Version 10, SAS Institute Inc., Cary, NC) to determine whether a gene was statistically significantly enriched. We used this test to compare paired (by insertion site) Hopcount values of input and output for every gene. For this test, output Hopcount values were normalized to the input by multiplying the number of reads at each insertion site in the output by the ratio: total reads in the input/total reads in the output. For genes with fewer than 4 insertion sites, a *P*-value was not determined. Statistically significant *P*-values were considered less than 1.18×10^{-5} according to the Bonferonni correction. The *P*-value reported in Table 1 is an average of the three antibiotic selection conditions. A list of all FE_{gene} scores and *P*-values is shown in Table S1.

The + IPTG selection data was analysed using the same methods as for the -IPTG data in order to confirm putative repressors. However, we performed additional analyses at the transposon insertion level, as opposed to the gene level, in an attempt to identify putative activators of *xds*. Fold enrichment of individual transposon insertions ($FE_{insertion}$) was calculated for both genic and intergenic insertions and insertions were sorted in rank order of $FE_{insertion}$. To calculate $FE_{insertion}$, we first normalized the output Hopcount values to the input as described above. $FE_{insertion}$ was calculated as: normalized output reads/input reads at every insertion site. Any insertions present in genes identified in the selection without IPTG were discarded from the analysis. Additionally, insertions directly upstream of the *bla-neo* resistance markers were discarded. A list of the remaining insertions with $FE_{insertion}$ greater than fivefold are shown in the Table S2. Enriched insertions were considered of interest if they fulfilled the following requirements: (i) exhibiting greater than fivefold enrichment, (ii) at least two insertions in the same intergenic/genic region were enriched, and (iii) enriched insertions in the same region exhibit strand bias (i.e. orientation of the P_{tac} promoter) in the output, but not the input.

RNA purification and qRT-PCR

For RNA isolation from plate grown bacteria, fresh colonies from semi-confluent plates were scraped up in LB and adjusted to an $OD_{600} = 10$, and frozen in 25% glycerol at –80°C in 100 µl aliquots of ~ 10^9 CFU. Frozen aliquots were thawed and plated on LB plates at a density of ~ 10^9 CFU per plate and incubated at 37°C for 2 h. Bacteria were removed from the plates by resuspending in LB and diluted in two volumes of RNAprotect Bacteria Reagent (Qiagen). For RNA isolation from bacteria grown in MOPS media, bacteria were grown overnight and 0.25–1 ml of culture was mixed with two volumes of RNAprotect. If RNA was not isolated the same day, samples were centrifuged at room temperature and the pellets were stored at –80°C. RNA was isolated from the cells using the RNeasy Mini Kit (Qiagen).

Any contaminating DNA in the RNA prep was digested using the TURBO DNA-*free* kit (Ambion, Life Technologies). cDNA was synthesized from 0.25–1 µg of DNA-free RNA using an iScript cDNA Synthesis Kit (Bio-Rad). DNA contamination was assessed through the use of control samples lacking reverse transcriptase. cDNA was diluted fivefold in DEPC treated water and 5 µl was used as a template for qRT-PCR. SYBR green qRT-PCR was conducted as described previously (Pratt *et al.*, 2009). Refer to Table S3 for the primers used in these experiments. All Ct values were corrected for primer efficiency as determined by a standard curve using genomic DNA template. Transcript levels were normalized to the housekeeping gene, *rpoB*, and fold change over wild type was calculated.

Recombination-based in vivo *expression technology (RIVET)*

Resolution assays were performed as described except that Kn was used in place of tetracycline (Pratt *et al.*, 2009). Additionally, for *in vivo* resolution analysis, 5-day-old CD-1 mice were intragastrically inoculated with plate grown bacteria, which were resuspended in LB. A single mouse received either 2×10^4 *xds–tnpR lacZ*::*res–neo–sacB–res* CFU ($OD_{600} = 0.001$) or 2×10^7 Δ*phoB xds–tnpR lacZ*::*res–neo–sacB–res* CFU ($OD_{600} = 0.5$). The higher dose for the latter strain was necessary due to its attenuated colonization phenotype. For the time-course RIVET experiment, *xds–tnpR lacZ*::*res–neo–sacB–res* was grown to mid-exponential phase in LB broth ($OD_{600} = 0.3$), washed twice in MOPS minimal medium (no phosphate added), and resuspended to an $OD_{600} = 0.001$. Mice were intragastically inoculated with 50 µl of the prepared inoculum. Mice were euthanized in groups of 4 or 5 at hours post inoculation: 4, 8, 12, 16, 20 and 24. Resolution was assessed as described above. For *in vitro* control, four independent inoculums were prepared the same way as described above. Resolution was measured in half hour increments for 4 h.

Evaluation of xds in vivo *fitness*

Bacterial inocula were prepared as described for the RIVET time-course experiment except that wild type and Δ*xds* strains were resuspended in MOPS containing either 0 or 10 mM KH_2PO_4 to an $OD_{600} = 0.005$. Five-day-old CD-1 mice were intragastrically inoculated with 50 µl of inocula. Eight hours post inoculation, the bacterial load in the infant mouse small intestine was assessed by homogenizing the small

intestine in 1 ml of LB + 20% glycerol and plating dilutions on LB + Sm plates. Each inoculum was tested in at least 8 mice using single strain infections.

Ethics statement

All animal experiments were done in accordance with NIH guidelines, the Animal Welfare Act and US federal law. Tufts University School of Medicine's Institutional Animal Care and Use Committee approved the experimental protocol 'B2013-44' that was used for this study. All animals were housed in a centralized and AAALAC-accredited research animal facility that is fully staffed with trained husbandry, technical and veterinary personnel.

Acknowledgements

The authors thank the Tufts University Core Facility for sequencing and computational support, as well as Bharathi Patimalla-Dipali for her gracious help with mouse experiments. This work was supported by US National Institutes of Health grants AI055058 (A.C.). A.C. is a Howard Hughes Medical Institute investigator.

References

Blanco, A.G., Canals, A., Bernues, J., Sola, M., and Coll, M. (2011) The structure of a transcription activation subcomplex reveals how sigma(70) is recruited to PhoB promoters. *EMBO J* **30:** 3776–3785.

Blankenberg, D., Von Kuster, G., Coraor, N., Ananda, G., Lazarus, R., Mangan, M., *et al*. (2010) Galaxy: a web-based genome analysis tool for experimentalists. *Curr Protoc Mol Biol* **Chapter 19:** Unit 19 10 11–Unit 19 10 21.

Cameron, D.E., Urbach, J.M., and Mekalanos, J.J. (2008) A defined transposon mutant library and its use in identifying motility genes in *Vibrio cholerae*. *Proc Natl Acad Sci USA* **105:** 8736–8741.

Camilli, A., and Mekalanos, J.J. (1995) Use of recombinase gene fusions to identify *Vibrio cholerae* genes induced during infection. *Mol Microbiol* **18:** 671–683.

Chao, M.C., Pritchard, J.R., Zhang, Y.J., Rubin, E.J., Livny, J., Davis, B.M., and Waldor, M.K. (2013) High-resolution definition of the *Vibrio cholerae* essential gene set with hidden Markov model-based analyses of transposon-insertion sequencing data. *Nucleic Acids Res* **41:** 9033–9048.

Childers, B.M., and Klose, K.E. (2007) Regulation of virulence in *Vibrio cholerae*: the ToxR regulon. *Future Microbiol* **2:** 335–344.

Diniz, M.M., Goulart, C.L., Barbosa, L.C., Farache, J., Lery, L.M., Pacheco, A.B., *et al*. (2011) Fine-tuning control of *phoBR* expression in *Vibrio cholerae* by binding of PhoB to multiple *pho* boxes. *J Bacteriol* **193:** 6929–6938.

DiRita, V.J. (1992) Co-ordinate expression of virulence genes by ToxR in *Vibrio cholerae*. *Mol Microbiol* **6:** 451–458.

Ferrieres, L., Hemery, G., Nham, T., Guerout, A.M., Mazel, D., Beloin, C., and Ghigo, J.M. (2010) Silent mischief: bacteriophage Mu insertions contaminate products of *Escherichia coli* random mutagenesis performed using suicidal transposon delivery plasmids mobilized by broad-host-range RP4 conjugative machinery. *J Bacteriol* **192:** 6418–6427.

Focareta, T., and Manning, P.A. (1987) Extracellular proteins of *Vibrio cholerae*: molecular cloning, nucleotide sequence and characterization of the deoxyribonuclease (DNase) together with its periplasmic localization in *Escherichia coli* K-12. *Gene* **53:** 31–40.

Focareta, T., and Manning, P.A. (1991a) Distinguishing between the extracellular DNases of *Vibrio cholerae* and development of a transformation system. *Mol Microbiol* **5:** 2547–2555.

Focareta, T., and Manning, P.A. (1991b) Genetic analysis of the export of an extracellular DNase of *Vibrio cholerae* using DNase-beta-lactamase fusions. *Gene* **108:** 31–37.

Furste, J.P., Pansegrau, W., Frank, R., Blocker, H., Scholz, P., Bagdasarian, M., and Lanka, E. (1986) Molecular cloning of the plasmid RP4 primase region in a multi-host-range *tacP* expression vector. *Gene* **48:** 119–131.

Giardine, B., Riemer, C., Hardison, R.C., Burhans, R., Elnitski, L., Shah, P., *et al*. (2005) Galaxy: a platform for interactive large-scale genome analysis. *Genome Res* **15:** 1451–1455.

Goecks, J., Nekrutenko, A., and Taylor, J. (2010) Galaxy: a comprehensive approach for supporting accessible, reproducible, and transparent computational research in the life sciences. *Genome Biol* **11:** R86.

Kamp, H.D., Patimalla-Dipali, B., Lazinski, D.W., Wallace-Gadsden, F., and Camilli, A. (2013) Gene fitness landscapes of *Vibrio cholerae* at important stages of its life cycle. *PLoS Pathog* **9:** e1003800.

Klein, B.A., Tenorio, E.L., Lazinski, D.W., Camilli, A., Duncan, M.J., and Hu, L.T. (2012) Identification of essential genes of the periodontal pathogen *Porphyromonas gingivalis*. *BMC Genomics* **13:** 578.

Kovacikova, G., and Skorupski, K. (2002) Regulation of virulence gene expression in *Vibrio cholerae* by quorum sensing: HapR functions at the *aphA* promoter. *Mol Microbiol* **46:** 1135–1147.

von Kruger, W.M., Humphreys, S., and Ketley, J.M. (1999) A role for the PhoBR regulatory system homologue in the *Vibrio cholerae* phosphate-limitation response and intestinal colonization. *Microbiology* **145:** 2463–2475.

Lamarche, M.G., Wanner, B.L., Crepin, S., and Harel, J. (2008) The phosphate regulon and bacterial virulence: a regulatory network connecting phosphate homeostasis and pathogenesis. *FEMS Microbiol Rev* **32:** 461–473.

Larocque, R.C., Harris, J.B., Dziejman, M., Li, X., Khan, A.I., Faruque, A.S., *et al*. (2005) Transcriptional profiling of *Vibrio cholerae* recovered directly from patient specimens during early and late stages of human infection. *Infect Immun* **73:** 4488–4493.

Lazinski, D.W., and Camilli, A. (2013) Homopolymer tail-mediated ligation PCR: a streamlined and highly efficient method for DNA cloning and library construction. *Biotechniques* **54:** 25–34.

Lee, S.H., Hava, D.L., Waldor, M.K., and Camilli, A. (1999) Regulation and temporal expression patterns of *Vibrio cholerae* virulence genes during infection. *Cell* **99:** 625–634.

Lipp, E.K., Huq, A., and Colwell, R.R. (2002) Effects of global

climate on infectious disease: the cholera model. *Clin Microbiol Rev* **15:** 757–770.
Lombardo, M.J., Michalski, J., Martinez-Wilson, H., Morin, C., Hilton, T., Osorio, C.G., *et al*. (2007) An *in vivo* expression technology screen for *Vibrio cholerae* genes expressed in human volunteers. *Proc Natl Acad Sci USA* **104:** 18229–18234.
Majumdar, A., Ghatak, A., and Ghosh, R.K. (2005) Identification of the gene for the monomeric alkaline phosphatase of *Vibrio cholerae* serogroup O1 strain. *Gene* **344:** 251–258.
Makino, K., Amemura, M., Kim, S.K., Nakata, A., and Shinagawa, H. (1993) Role of the sigma 70 subunit of RNA polymerase in transcriptional activation by activator protein PhoB in *Escherichia coli*. *Genes Dev* **7:** 149–160.
Mandlik, A., Livny, J., Robins, W.P., Ritchie, J.M., Mekalanos, J.J., and Waldor, M.K. (2011) RNA-Seq-based monitoring of infection-linked changes in *Vibrio cholerae* gene expression. *Cell Host Microbe* **10:** 165–174.
Mekalanos, J.J. (1983) Duplication and amplification of toxin genes in *Vibrio cholerae*. *Cell* **35:** 253–263.
Merrell, D.S., Hava, D.L., and Camilli, A. (2002) Identification of novel factors involved in colonization and acid tolerance of *Vibrio cholerae*. *Mol Microbiol* **43:** 1471–1491.
Merrell, D.S., Butler, S.M., Qadri, F., Dolganov, N.A., Alam, A., Cohen, M.B., *et al*. (2002) Host-induced epidemic spread of the cholera bacterium. *Nature* **417:** 642–645.
Miller, M.B., Skorupski, K., Lenz, D.H., Taylor, R.K., and Bassler, B.L. (2002) Parallel quorum sensing systems converge to regulate virulence in *Vibrio cholerae*. *Cell* **110:** 303–314.
Nelson, E.J., Chowdhury, A., Flynn, J., Schild, S., Bourassa, L., Shao, Y., *et al*. (2008) Transmission of *Vibrio cholerae* is antagonized by lytic phage and entry into the aquatic environment. *PLoS Pathog* **4:** e1000187.
Newland, J.W., Green, B.A., Foulds, J., and Holmes, R.K. (1985) Cloning of extracellular DNase and construction of a DNase-negative strain of *Vibrio cholerae*. *Infect Immun* **47:** 691–696.
Nielsen, A.T., Dolganov, N.A., Otto, G., Miller, M.C., Wu, C.Y., and Schoolnik, G.K. (2006) RpoS controls the *Vibrio cholerae* mucosal escape response. *PLoS Pathog* **2:** e109.
Nielsen, A.T., Dolganov, N.A., Rasmussen, T., Otto, G., Miller, M.C., Felt, S.A., *et al*. (2010) A bistable switch and anatomical site control *Vibrio cholerae* virulence gene expression in the intestine. *PLoS Pathog* **6:** e1001102.
van Opijnen, T., Bodi, K.L., and Camilli, A. (2009) Tn-seq: high-throughput parallel sequencing for fitness and genetic interaction studies in microorganisms. *Nat Methods* **6:** 767–772.
Osorio, C.G., Crawford, J.A., Michalski, J., Martinez-Wilson, H., Kaper, J.B., and Camilli, A. (2005) Second-generation recombination-based *in vivo* expression technology for large-scale screening for *Vibrio cholerae* genes induced during infection of the mouse small intestine. *Infect Immun* **73:** 972–980.
Peterson, K.M. (2002) Expression of *Vibrio cholerae* virulence genes in response to environmental signals. *Curr Issues Intest Microbiol* **3:** 29–38.
Pratt, J.T., McDonough, E., and Camilli, A. (2009) PhoB regulates motility, biofilms, and cyclic di-GMP in *Vibrio cholerae*. *J Bacteriol* **191:** 6632–6642.
Pratt, J.T., Ismail, A.M., and Camilli, A. (2010) PhoB regulates both environmental and virulence gene expression in *Vibrio cholerae*. *Mol Microbiol* **77:** 1595–1605.
Schild, S., Tamayo, R., Nelson, E.J., Qadri, F., Calderwood, S.B., and Camilli, A. (2007) Genes induced late in infection increase fitness of *Vibrio cholerae* after release into the environment. *Cell Host Microbe* **2:** 264–277.
Seper, A., Fengler, V.H., Roier, S., Wolinski, H., Kohlwein, S.D., Bishop, A.L., *et al*. (2011) Extracellular nucleases and extracellular DNA play important roles in *Vibrio cholerae* biofilm formation. *Mol Microbiol* **82:** 1015–1037.
Seper, A., Hosseinzadeh, A., Gorkiewicz, G., Lichtenegger, S., Roier, S., Leitner, D.R., *et al*. (2013) *Vibrio cholerae* evades neutrophil extracellular traps by the activity of two extracellular nucleases. *PLoS Pathog* **9:** e1003614.
Zhu, J., and Mekalanos, J.J. (2003) Quorum sensing-dependent biofilms enhance colonization in *Vibrio cholerae*. *Dev Cell* **5:** 647–656.
Zhu, J., Miller, M.B., Vance, R.E., Dziejman, M., Bassler, B.L., and Mekalanos, J.J. (2002) Quorum-sensing regulators control virulence gene expression in *Vibrio cholerae*. *Proc Natl Acad Sci USA* **99:** 3129–3134.

Supporting information

Additional supporting information may be found in the online version of this article at the publisher's web-site.